

Measurement of the energy spectrum of
cosmic rays above 10^{18} eV using the Pierre
Auger Observatory.
arXiv:1002.1975v1

Outline

- 1 General background
- 2 Detection and Analysis
 - Detectors
 - Analysis
- 3 Results and conclusions
 - Conclusions

Outline

- 1 General background
- 2 Detection and Analysis
 - Detectors
 - Analysis
- 3 Results and conclusions
 - Conclusions

Outline

- 1 General background
- 2 Detection and Analysis
 - Detectors
 - Analysis
- 3 Results and conclusions
 - Conclusions

General Background



- The Ultra High Energy Cosmic Rays (UHECR), are the most energetic and rarest of particles studied in Pierre Auger. Billions of secondary particles (shower) are produced when they strike the atmosphere.
- Flux of UHECRs exhibits:
 - 1 above 4×10^{19} eV a suppression of flux with respect to the power law, compatible with GZK effect.
 - 2 Break in power law (ankle) observed $\approx 4 \times 10^{18}$ eV

General Background



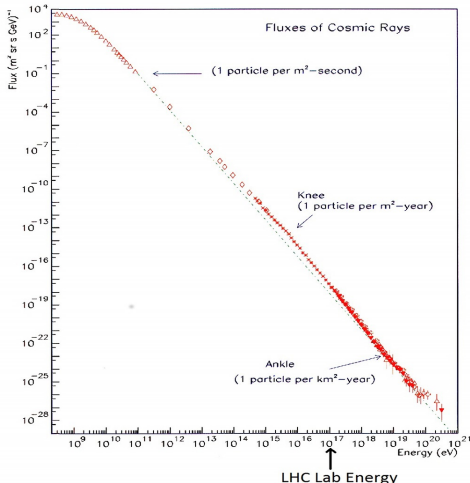
- The Ultra High Energy Cosmic Rays (UHECR), are the most energetic and rarest of particles are studied in Pierre Auger. Billions of secondary particles (shower) are produced when they strike the atmosphere.
- Flux of UHECRs exhibits:
 - 1 above 4×10^{19} eV a suppression of flux with respect to the power law, compatible with GZK effect.
 - 2 Break in power law (ankle) observed $\approx 4 \times 10^{18}$ eV

General Background



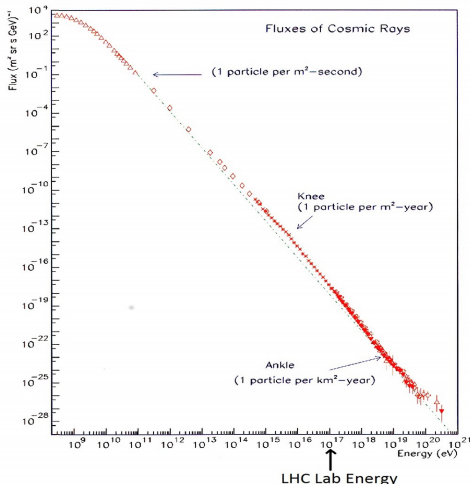
- The Ultra High Energy Cosmic Rays (UHECR), are the most energetic and rarest of particles are studied in Pierre Auger. Billions of secondary particles (shower) are produced when they strike the atmosphere.
- Flux of UHECRs exhibits:
 - 1 above 4×10^{19} eV a suppression of flux with respect to the power law, compatible with GZK effect.
 - 2 Break in power law (ankle) observed $\approx 4 \times 10^{18}$ eV

The Cosmic Ray spectrum



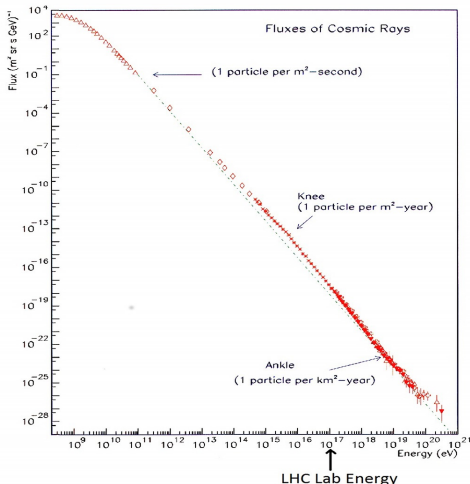
- Spectrum defined by broken power law.
- Knee at $E \sim 4 \text{ PeV}$.
- Ankle at $E \sim 4 \text{ EeV}$ (galactic to extragalactic CR?).
- GZK Cutoff predicted to be at $E \sim 50 \text{ EeV}$.

The Cosmic Ray spectrum



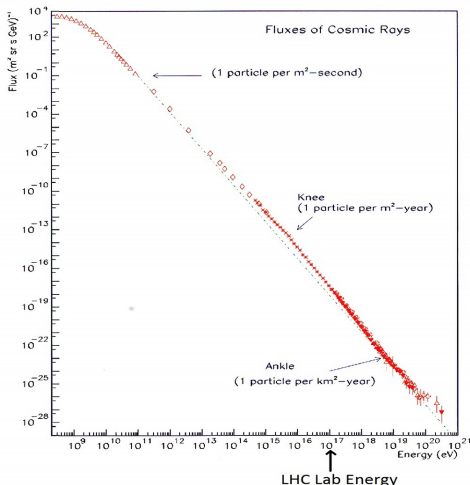
- Spectrum defined by broken power law.
- Knee at $E \sim 4 \text{ PeV}$.
- Ankle at $E \sim 4 \text{ EeV}$ (galactic to extragalactic CR?).
- GZK Cutoff predicted to be at $E \sim 50 \text{ EeV}$.

The Cosmic Ray spectrum



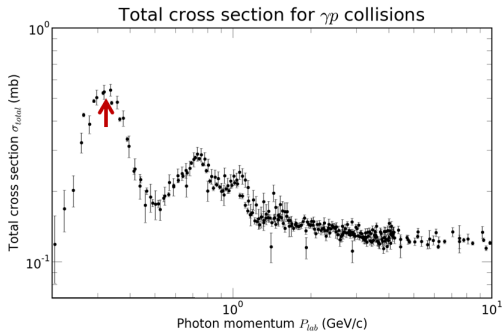
- Spectrum defined by broken power law.
- Knee at $E \sim 4 \text{ PeV}$.
- Ankle at $E \sim 4 \text{ EeV}$ (galactic to extragalactic CR?).
- GZK Cutoff predicted to be at $E \sim 50 \text{ EeV}$.

The Cosmic Ray spectrum



- Spectrum defined by broken power law.
- Knee at $E \sim 4 \text{ PeV}$.
- Ankle at $E \sim 4 \text{ EeV}$ (galactic to extragalactic CR?).
- GZK Cutoff predicted to be at $E \sim 50 \text{ EeV}$.

The Greisen-Zatsepin-Kuzmin (GZK) Cutoff



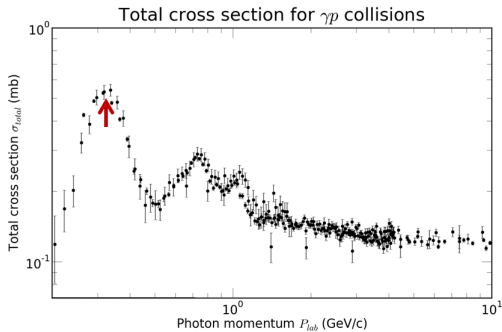
Taken from PDG

- Greisen-Zatsepin-Kuzmin cutoff is the result of photo-pion production.
- Main process: proton collision with Cosmic Microwave Background (CMB) photon.



- Cross section enhanced by $\Delta^+(1232)$ -resonance.

The Greisen-Zatsepin-Kuzmin (GZK) Cutoff



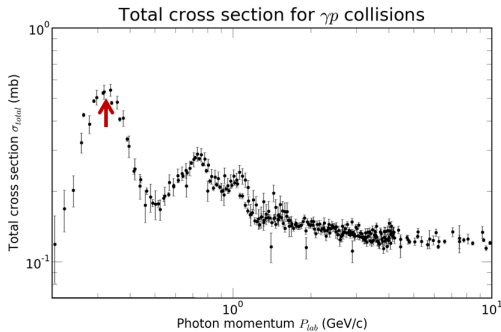
Taken from PDG

- Greisen-Zatsepin-Kuzmin cutoff is the result of photo-pion production.
- Main process: proton collision with Cosmic Microwave Background (CMB) photon.



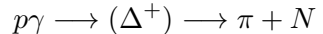
- Cross section enhanced by $\Delta^+(1232)$ -resonance.

The Greisen-Zatsepin-Kuzmin (GZK) Cutoff



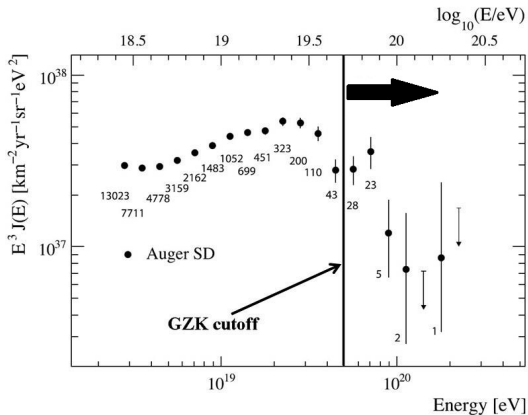
Taken from PDG

- Greisen-Zatsepin-Kuzmin cutoff is the result of photo-pion production.
- Main process: proton collision with Cosmic Microwave Background (CMB) photon.



- Cross section enhanced by $\Delta^+(1232)$ -resonance.

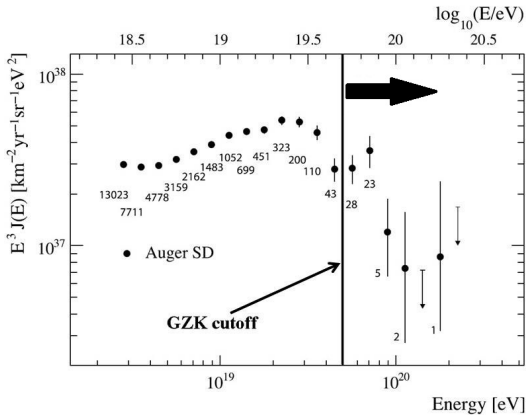
GZK Cutoff



Taken from The Pierre Auger Collaboration, arXiv: 1002.1975v1

- Proton energy loss leads to cutoff at 10^{20} eV.
- Mean interaction length $\approx 10 \text{ Mpc}$.
- “GZK Horizon” at 50 Mpc, no 10^{20} eV particles past this distance.

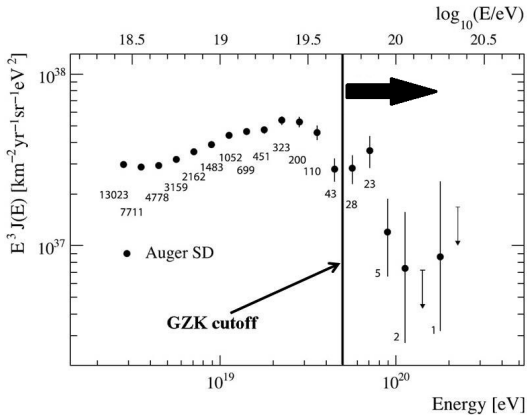
GZK Cutoff



Taken from The Pierre Auger Collaboration, arXiv: 1002.1975v1

- Proton energy loss leads to cutoff at 10^{20} eV.
- Mean interaction length $\approx 10 \text{ Mpc}$.
- “GZK Horizon” at 50 Mpc, no 10^{20} eV particles past this distance.

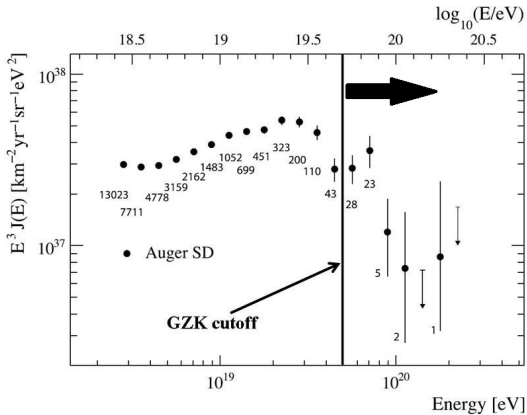
GZK Cutoff



Taken from The Pierre Auger Collaboration, arXiv: 1002.1975v1

- Proton energy loss leads to cutoff at 10^{20} eV.
- Mean interaction length $\approx 10 \text{ Mpc}$.
- “GZK Horizon” at 50 Mpc, no 10^{20} eV particles past this distance.

GZK Cutoff



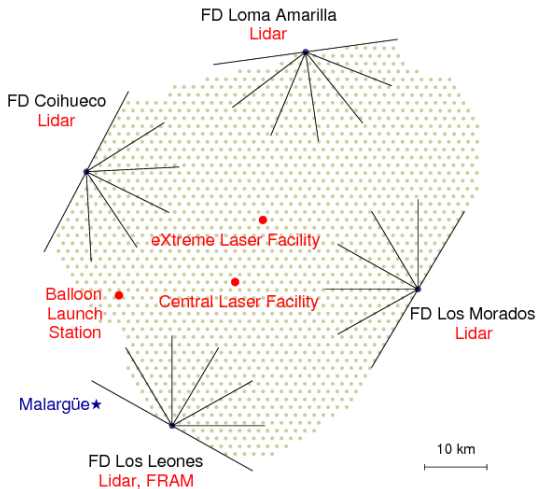
Taken from The Pierre Auger Collaboration, arXiv: 1002.1975v1

- Proton energy loss leads to cutoff at 10^{20} eV.
- Mean interaction length $\approx 10 \text{ Mpc}$.
- “GZK Horizon” at 50 Mpc, no 10^{20} eV particles past this distance.

Outline

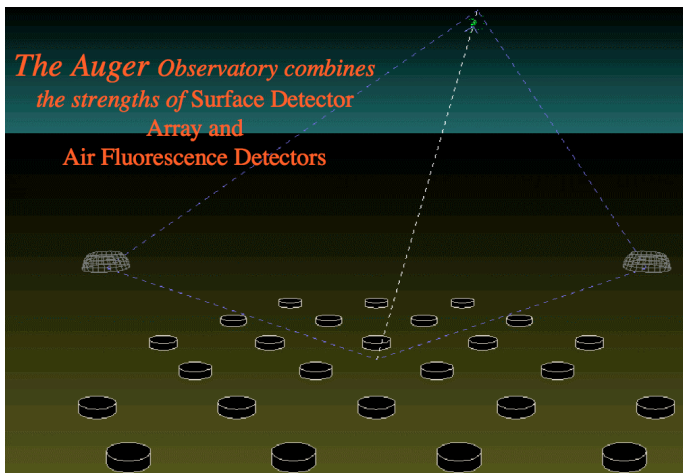
- 1 General background
- 2 **Detection and Analysis**
 - Detectors
 - Analysis
- 3 Results and conclusions
 - Conclusions

The Pierre Auger Experiment



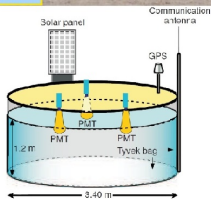
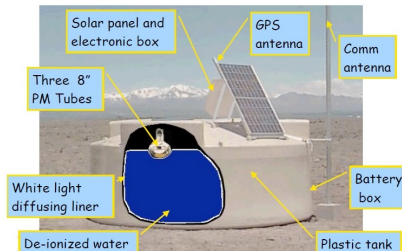
Taken from *The Pierre Auger Collaboration, arXiv: 1002.0366 [astro-ph.HE] 2010*

The Detectors of Pierre Auger Experiment



Taken from icecube.wisc.edu/~tmontaruli/801/lect17.pdf

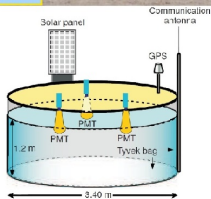
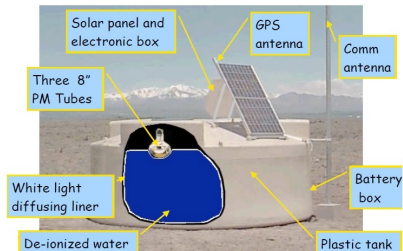
The Surface Detectors (SD) (general information)



Taken from www.lip.pt/~jespada/Research/PAO.php

- 1600 water-Cherenkov detectors, distributed over 3000 km^2 , spaced 1.5 km on a triangular grid.
- Dimensions: $3.6\text{m diam} \times 1.5\text{m height}$.
- 12 tons of pure water per tank.
- 3 PMT detectors per tank, distributed symmetrically from center of tank.

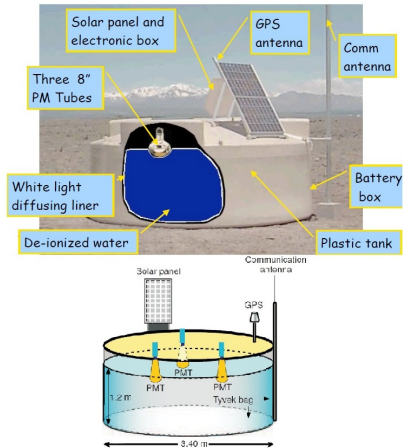
The Surface Detectors (SD) (general information)



Taken from www.lip.pt/~jespada/Research/PAO.php

- 1600 water-Cherenkov detectors, distributed over 3000 km^2 , spaced 1.5 km on a triangular grid.
- Dimensions: $3.6 \text{ m diam} \times 1.5 \text{ m height}$.
- 12 tons of pure water per tank.
- 3 PMT detectors per tank, distributed symmetrically from center of tank.

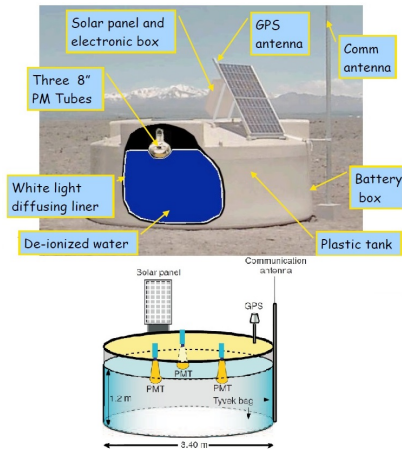
The Surface Detectors (SD) (general information)



Taken from www.lip.pt/~jespada/Research/PAO.php

- 1600 water-Cherenkov detectors, distributed over 3000 km^2 , spaced 1.5 km on a triangular grid.
- Dimensions: $3.6 \text{ m diam} \times 1.5 \text{ m height}$.
- 12 tons of pure water per tank.
- 3 PMT detectors per tank, distributed symmetrically from center of tank.

The Surface Detectors (SD) (general information)



Taken from www.lip.pt/~jespada/Research/PAO.php

- 1600 water-Cherenkov detectors, distributed over 3000 km^2 , spaced 1.5 km on a triangular grid.
- Dimensions: $3.6 \text{ m diam} \times 1.5 \text{ m height}$.
- 12 tons of pure water per tank.
- 3 PMT detectors per tank, distributed symmetrically from center of tank.

The SD Detector (Trigger)

- Five triggers.
- T1 (local): Time-over-threshold (ToT).
- T2 (local): Single threshold.
- T3 (array): Coincidence in > 3 stations which passed the T2 trigger.
- T4 (physics): One station and 3 direct neighbours passed the T3 trigger.
- T5 (quality): Station with highest signal must have all six neighbouring stations active.

The SD Detector (Trigger)

- Five triggers.
- T1 (local): Time-over-threshold (ToT).
- T2 (local): Single threshold.
- T3 (array): Coincidence in > 3 stations which passed the T2 trigger.
- T4 (physics): One station and 3 direct neighbours passed the T3 trigger.
- T5 (quality): Station with highest signal must have all six neighbouring stations active.

The SD Detector (Trigger)

- Five triggers.
- T1 (local): Time-over-threshold (ToT).
- T2 (local): Single threshold.
- T3 (array): Coincidence in > 3 stations which passed the T2 trigger.
- T4 (physics): One station and 3 direct neighbours passed the T3 trigger.
- T5 (quality): Station with highest signal must have all six neighbouring stations active.

The SD Detector (Trigger)

- Five triggers.
- T1 (local): Time-over-threshold (ToT).
- T2 (local): Single threshold.
- T3 (array): Coincidence in > 3 stations which passed the T2 trigger.
- T4 (physics): One station and 3 direct neighbours passed the T3 trigger.
- T5 (quality): Station with highest signal must have all six neighbouring stations active.

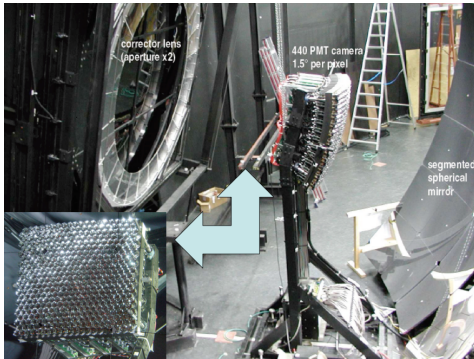
The SD Detector (Trigger)

- Five triggers.
- T1 (local): Time-over-threshold (ToT).
- T2 (local): Single threshold.
- T3 (array): Coincidence in > 3 stations which passed the T2 trigger.
- T4 (physics): One station and 3 direct neighbours passed the T3 trigger.
- T5 (quality): Station with highest signal must have all six neighbouring stations active.

The SD Detector (Trigger)

- Five triggers.
- T1 (local): Time-over-threshold (ToT).
- T2 (local): Single threshold.
- T3 (array): Coincidence in > 3 stations which passed the T2 trigger.
- T4 (physics): One station and 3 direct neighbours passed the T3 trigger.
- T5 (quality): Station with highest signal must have all six neighbouring stations active.

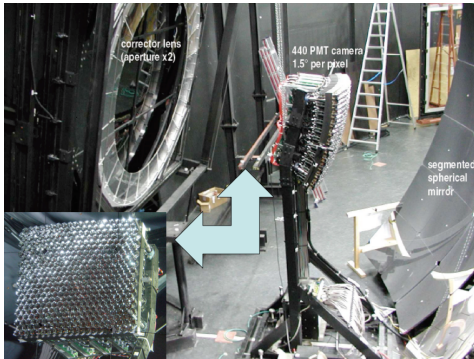
The fluorescence detectors (FD)



Taken from icecube.wisc.edu/~tmontaruli/801/lect17.pdf

- Measure the longitudinal profile of the shower dE/dX . (calorimetric)
- Duty cycle of about 10%, works on clear nights only.
- Calibration of SD energy estimator.
- N_2 excitation emit light in the 300 – 430 nm range. # Photons \propto to the energy deposited.

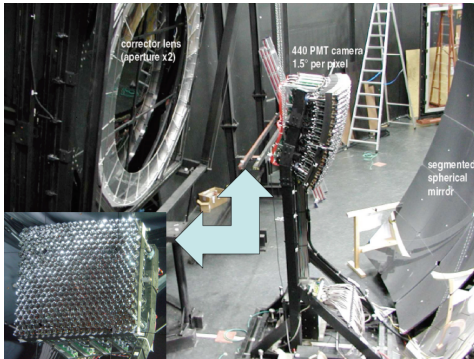
The fluorescence detectors (FD)



Taken from icecube.wisc.edu/~tmontaruli/801/lect17.pdf

- Measure the longitudinal profile of the shower dE/dX . (calorimetric)
- Duty cycle of about 10%, works on clear nights only.
- Calibration of SD energy estimator.
- N_2 excitation emit light in the 300 – 430 nm range. # Photons \propto to the energy deposited.

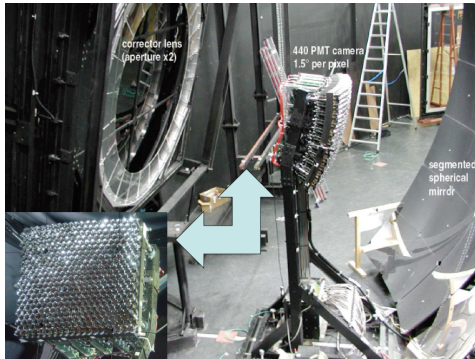
The fluorescence detectors (FD)



Taken from icecube.wisc.edu/~tmontaruli/801/lect17.pdf

- Measure the longitudinal profile of the shower dE/dX . (calorimetric)
- Duty cycle of about 10%, works on clear nights only.
- Calibration of SD energy estimator.
- N_2 excitation emit light in the 300 – 430 nm range. # Photons \propto to the energy deposited.

The fluorescence detectors (FD)



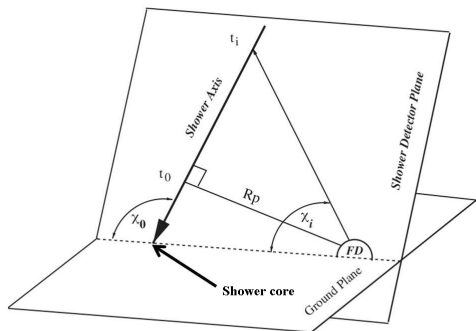
Taken from icecube.wisc.edu/~tmontaruli/801/lect17.pdf

- Measure the longitudinal profile of the shower dE/dX . (calorimetric)
- Duty cycle of about 10%, works on clear nights only.
- Calibration of SD energy estimator.
- N_2 excitation emit light in the 300 – 430 nm range. # Photons \propto to the energy deposited.

Outline

- 1 General background
- 2 **Detection and Analysis**
 - Detectors
 - **Analysis**
- 3 Results and conclusions
 - Conclusions

Detection of the Shower-Detector Plane (SDP)

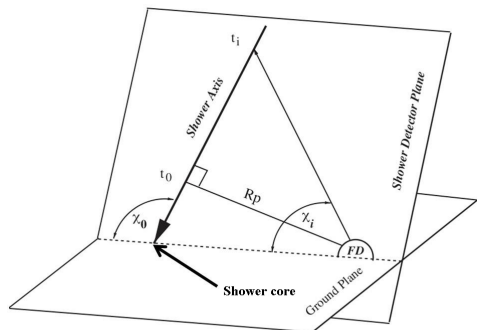


Taken from Nuclear Instruments & Methods in Physics Research, Properties and performance of the prototype instrument for the Pierre Auger Observatory (2003)

- Uncertainty in SDP
 $\sim 0.1^\circ$.
- Timing information of SD and FD used.
- Shower parameters (R_p, χ_0) are determined by fitting the timings and angles for all detectors to the functional form:

$$t_i = t_0 + \frac{R_p}{c} \tan \left(\frac{\chi_0 - \chi_i}{2} \right)$$

Detection of the Shower-Detector Plane (SDP)

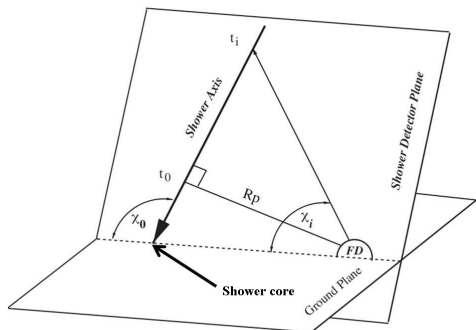


Taken from Nuclear Instruments & Methods in Physics Research, Properties and performance of the prototype instrument for the Pierre Auger Observatory (2003)

- Uncertainty in SDP
 $\sim 0.1^\circ$.
- Timing information of SD and FD used.
- Shower parameters (R_p, χ_0) are determined by fitting the timings and angles for all detectors to the functional form:

$$t_i = t_0 + \frac{R_p}{c} \tan \left(\frac{\chi_0 - \chi_i}{2} \right)$$

Detection of the Shower-Detector Plane (SDP)

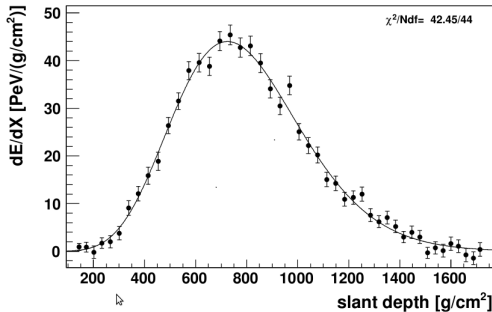


Taken from Nuclear Instruments & Methods in Physics Research, Properties and performance of the prototype instrument for the Pierre Auger Observatory (2003)

- Uncertainty in SDP
 $\sim 0.1^\circ$.
- Timing information of SD and FD used.
- Shower parameters (R_p, χ_0) are determined by fitting the timings and angles for all detectors to the functional form:

$$t_i = t_0 + \frac{R_p}{c} \tan \left(\frac{\chi_0 - \chi_i}{2} \right)$$

Energy reconstruction



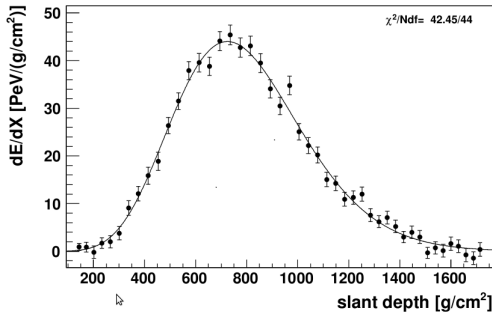
Taken from The Pierre Auger Collaboration, arXiv:0907.4282v1 [astro-ph.IM]

- slant depth

$$X^\mu = \int_z^\infty \rho(z') dz'$$

- The shower profile dE/dX is fitted to a Gaisser-Hillas function.
- An integration is performed to estimate the total shower energy.

Energy reconstruction



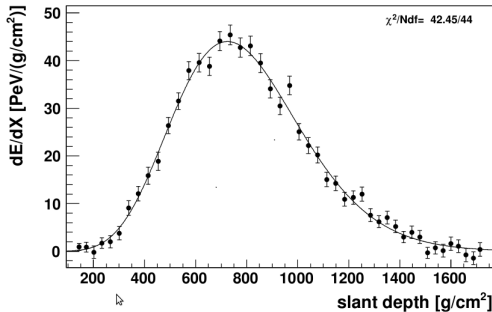
Taken from The Pierre Auger Collaboration, arXiv:0907.4282v1 [astro-ph.IM]

- slant depth

$$X^\mu = \int_z^\infty \rho(z') dz'$$

- The shower profile dE/dX is fitted to a Gaisser-Hillas function.
- An integration is performed to estimate the total shower energy.

Energy reconstruction



Taken from The Pierre Auger Collaboration, arXiv:0907.4282v1 [astro-ph.IM]

- slant depth

$$X^\mu = \int_z^\infty \rho(z') dz'$$

- The shower profile dE/dX is fitted to a Gaisser-Hillas function.
- An integration is performed to estimate the total shower energy.

Event Selection and Reconstruction

- Reconstructed showers with zenith angle $< 60^\circ$ and core must be within 1500 m of the station used for the geometrical reconstruction.
- Cherenkov light must contribute less than 50% of the overall FD signal.
- Gaisser-Hillas fit of the reconstructed profile must have $\chi^2/Ndof < 2.5$.
- X_{max} , must be in the field of view of the telescopes.
- Reconstructed energy must satisfy $\sigma(E)/E < 20\%$.

Event Selection and Reconstruction

- Reconstructed showers with zenith angle $< 60^\circ$ and core must be within 1500 m of the station used for the geometrical reconstruction.
- Cherenkov light must contribute less than 50% of the overall FD signal.
- Gaisser-Hillas fit of the reconstructed profile must have $\chi^2/Ndof < 2.5$.
- X_{max} , must be in the field of view of the telescopes.
- Reconstructed energy must satisfy $\sigma(E)/E < 20\%$.

Event Selection and Reconstruction

- Reconstructed showers with zenith angle $< 60^\circ$ and core must be within 1500 m of the station used for the geometrical reconstruction.
- Cherenkov light must contribute less than 50% of the overall FD signal.
- Gaisser-Hillas fit of the reconstructed profile must have $\chi^2/Ndof < 2.5$.
- X_{max} , must be in the field of view of the telescopes.
- Reconstructed energy must satisfy $\sigma(E)/E < 20\%$.

Event Selection and Reconstruction

- Reconstructed showers with zenith angle $< 60^\circ$ and core must be within 1500 m of the station used for the geometrical reconstruction.
- Cherenkov light must contribute less than 50% of the overall FD signal.
- Gaisser-Hillas fit of the reconstructed profile must have $\chi^2/Ndof < 2.5$.
- X_{max} , must be in the field of view of the telescopes.
- Reconstructed energy must satisfy $\sigma(E)/E < 20\%$.

Event Selection and Reconstruction

- Reconstructed showers with zenith angle $< 60^\circ$ and core must be within 1500 m of the station used for the geometrical reconstruction.
- Cherenkov light must contribute less than 50% of the overall FD signal.
- Gaisser-Hillas fit of the reconstructed profile must have $\chi^2/Ndof < 2.5$.
- X_{max} , must be in the field of view of the telescopes.
- Reconstructed energy must satisfy $\sigma(E)/E < 20\%$.

Exposure Calculation

Total Exposure:

$$\mathcal{E}(E) = \int_{(T)} \int_{\Omega} \int_{S_{gen}} \epsilon(E, t, \theta, \phi, x, y) \cos \theta dS d\Omega dt$$

Diagram illustrating the exposure calculation formula with annotations:

- Operating time**: points to the integration variable T .
- final selection efficiency**: points to the function ϵ .
- horizontal surface element**: points to the dS term.
- zenith angles**: points to the angle θ .
- azimuth angles**: points to the angle ϕ .

- Based on hadronic interaction models QGSJet-II and Sibyll 2.1.
- Air shower simulation using CONEX (MC).
- Atmospheric conditions taken into account.

Exposure Calculation

Total Exposure:

$$\mathcal{E}(E) = \int_{\mathcal{T}} \int_{\Omega} \int_{S_{gen}} \epsilon(E, t, \theta, \phi, x, y) \cos \theta dS d\Omega dt$$

Diagram illustrating the components of the exposure calculation equation:

- \mathcal{T} : Operating time
- Ω : Solid angle
- S_{gen} : Horizontal surface element
- $\epsilon(E, t, \theta, \phi, x, y)$: Final selection efficiency, where θ is the zenith angle and ϕ is the azimuth angle.
- $\cos \theta$: Geometric factor
- $dS d\Omega dt$: Differential volume element

- Based on hadronic interaction models QGSJet-II and Sibyll 2.1.
- Air shower simulation using CONEX (MC).
- Atmospheric conditions taken into account.

Exposure Calculation

Total Exposure:

$$\mathcal{E}(E) = \int_{(T)} \int_{\Omega} \int_{S_{gen}} \epsilon(E, t, \theta, \phi, x, y) \cos \theta dS d\Omega dt$$

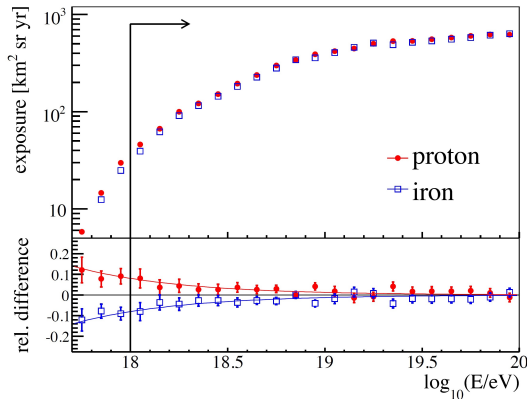
Diagram illustrating the components of the exposure calculation equation:

- Operating time**: Points to the integration over time (T) .
- final selection efficiency**: Points to the efficiency function $\epsilon(E, t, \theta, \phi, x, y)$.
- zenith angles**: Points to the angle θ .
- azimuth angles**: Points to the angle ϕ .
- horizontal surface element**: Points to the differential area element dS .

- Based on hadronic interaction models QGSJet-II and Sibyll 2.1.
- Air shower simulation using CONEX (MC).
- Atmospheric conditions taken into account.

Exposure calculation

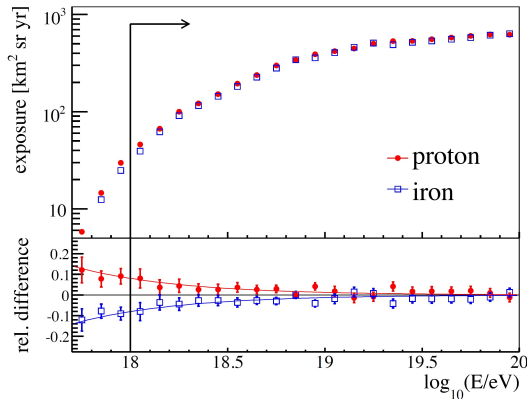
- Syst. Uncertainty for mass composition: 8% at $10^{18} eV$ and 1% at $10^{19} eV$
- 50% p and 50% iron.
- Exposure dependence on the hadronic model is less than 2%



Taken from *The Pierre Auger Collaboration, arXiv:1002.1975v1 [astro-ph.HE] 2010*

Exposure calculation

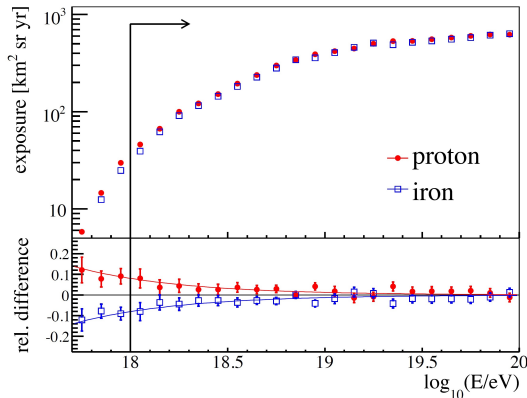
- Syst. Uncertainty for mass composition: 8% at $10^{18} eV$ and 1% at $10^{19} eV$
- 50% p and 50% iron.
- Exposure dependence on the hadronic model is less than 2%



Taken from *The Pierre Auger Collaboration, arXiv:1002.1975v1 [astro-ph.HE] 2010*

Exposure calculation

- Syst. Uncertainty for mass composition: 8% at $10^{18} eV$ and 1% at $10^{19} eV$
- 50% p and 50% iron.
- Exposure dependence on the hadronic model is less than 2%



Taken from *The Pierre Auger Collaboration, arXiv:1002.1975v1 [astro-ph.HE] 2010*

Flux calculation

Flux of cosmic rays

Number of cosmic rays with incident energy E

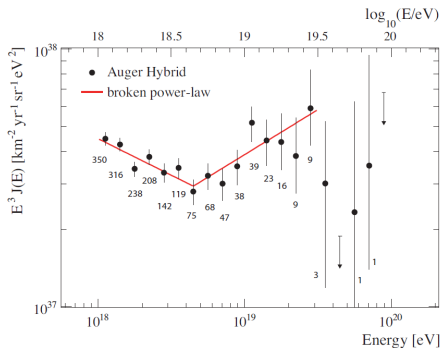
Number of detected events passing the quality cuts

Energy dependent-exposure

$$J(E) = \frac{d^4 N_{inc}}{dE dA d\Omega dt} \approx \frac{\Delta N_{sel}(E)}{\Delta E} \frac{1}{\mathcal{E}(E)}$$

Approx. is made using the total exposure function \mathcal{E} and $\Delta N_{sel}(E)$ which is the number of selected events.

Hybrid data parameters



Taken from The Pierre Auger Collaboration, arXiv:1002.1975v1 [astro-ph.HE] 2010

- Ankle

$$\log_{10} \frac{E_{ankle}}{eV} = 18.65 \pm 0.09 (stat) \pm 0.10 (sys) - 0.11 (sys)$$

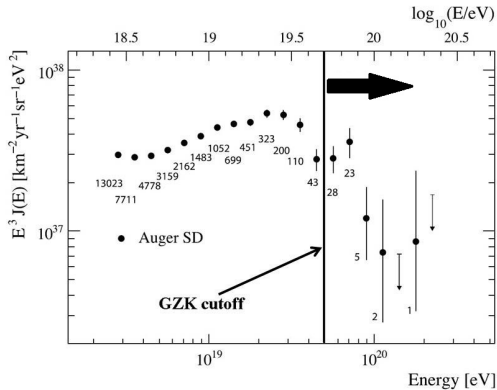
- Power law indices

- $\gamma_1 = 3.28 \pm 0.07 (stat) \pm 0.11 (sys) - 0.10 (sys)$

- $\gamma_2 = 2.65 \pm 0.14 (stat) \pm 0.16 (sys) - 0.14 (sys)$

- Syst uncert \rightarrow effect of the unknown mass composition

Update of the SD spectrum



Taken from The Pierre Auger Collaboration, arXiv: 1002.1975v1

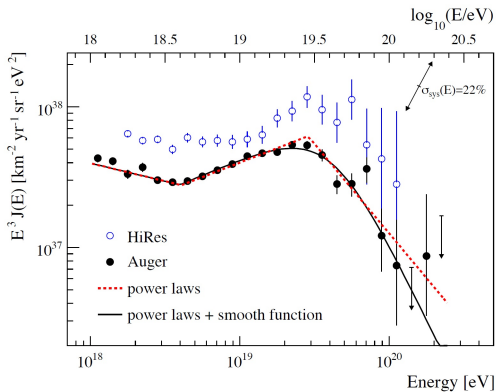
- Data update based on SD data until Dec 2008.
- Current exposure 12790 $\text{Km}^2 \text{sr yr}$.
- Energy estimator of the SD is corrected for shower attenuation effects using a constant intensity method.

Combined Auger Spectrum

- To combine hybrid and updated SD data, the scale parameter k is used to match the difference between the two sets of data.
- The function at higher energies is given by

$$J(E; E > E_{ankle}) \propto \frac{E^{-\gamma_2}}{1 + e^{\frac{\log_{10}(E) - \log_{10} E_{1/2}}{\log_{10}(W_e)}}}$$

Combined energy spectrum and fitted parameters and statistical uncertainties.



parameter	power laws	power laws + smooth function
$\gamma_1(E < E_{\text{ankle}})$	3.26 ± 0.04	3.26 ± 0.04
$\log_{10}(E_{\text{ankle}}/\text{eV})$	18.61 ± 0.01	18.60 ± 0.01
$\gamma_2(E > E_{\text{ankle}})$	2.59 ± 0.02	2.55 ± 0.04
$\log_{10}(E_{\text{break}}/\text{eV})$	19.46 ± 0.03	
$\gamma_3(E > E_{\text{break}})$	4.3 ± 0.2	
$\log_{10}(E_{1/2}/\text{eV})$		19.61 ± 0.03
$\log_{10}(W_c/\text{eV})$		0.16 ± 0.03
χ^2/ndof	$38.5/16$	$29.1/16$

Taken from The Pierre Auger Collaboration, arXiv:1002.1975v1 [astro-ph.HE] 2010

Outline

- 1 General background
- 2 Detection and Analysis
 - Detectors
 - Analysis
- 3 Results and conclusions
 - Conclusions

Conclusions

- The CR flux has been measured with the Pierre Auger Observatory by applying two different techniques.
- Good agreement in the overlapping energy range.
- A combined spectrum has been derived covering energy range $10^{18}eV - 10^{20}eV$.



$$\gamma = \left\{ \begin{array}{ll} 3.26 \pm 0.04 & \text{below the ankle,} \\ 2.55 \pm 0.04 & \text{above the ankle} \end{array} \right\}$$

- Suppression is similar to what is expected from GZK effect.

Conclusions

- The CR flux has been measured with the Pierre Auger Observatory by applying two different techniques.
- Good agreement in the overlapping energy range.
- A combined spectrum has been derived covering energy range $10^{18} eV - 10^{20} eV$.



$$\gamma = \left\{ \begin{array}{ll} 3.26 \pm 0.04 & \text{below the ankle,} \\ 2.55 \pm 0.04 & \text{above the ankle} \end{array} \right\}$$

- Suppression is similar to what is expected from GZK effect.

Conclusions

- The CR flux has been measured with the Pierre Auger Observatory by applying two different techniques.
- Good agreement in the overlapping energy range.
- A combined spectrum has been derived covering energy range $10^{18}eV - 10^{20}eV$.



$$\gamma = \left\{ \begin{array}{ll} 3.26 \pm 0.04 & \text{below the ankle,} \\ 2.55 \pm 0.04 & \text{above the ankle} \end{array} \right\}$$

- Suppression is similar to what is expected from GZK effect.

Conclusions

- The CR flux has been measured with the Pierre Auger Observatory by applying two different techniques.
- Good agreement in the overlapping energy range.
- A combined spectrum has been derived covering energy range $10^{18}eV - 10^{20}eV$.



$$\gamma = \left\{ \begin{array}{ll} 3.26 \pm 0.04 & \text{below the ankle,} \\ 2.55 \pm 0.04 & \text{above the ankle} \end{array} \right\}$$

- Suppression is similar to what is expected from GZK effect.

Group E Collaboration - CLASHEP 2013



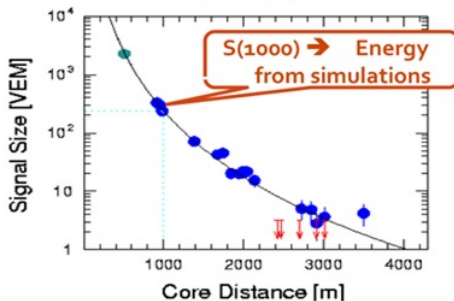
Backup slide

About the Energy estimator:

$$S(r) = S(1000) \left(\frac{r}{1000} \right)^{-\beta} \left(\frac{r + 700}{1700} \right)^{-\beta}$$

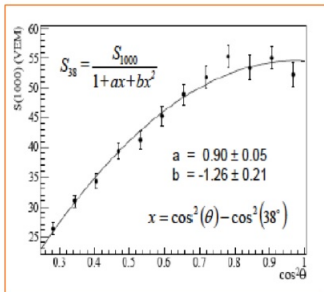
Lateral density distribution

ID 762238



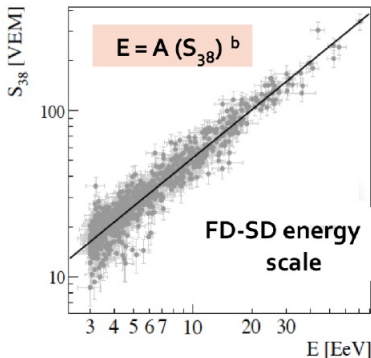
Taken from M. Dova - CLASHEP 2013.

Backup slide



Zenith angle dependence
 of s_{1000}

Taken from M. Dova - CLASHEP 2013.



Backup slide

- The normalization uncertainties are used as additional constraints in the combination.
- The combination is procedure used the scale parameter k .
- The parameter k , is precisely the difference between the two measurements.
- The equation 2 is another model function which unifies the two higher energy ranges such as that the change in the energy not change abrupt in 2×10^{19} eV.
- The combined energy spectrum if fitted with two functions and compared to data from the HiRes instrument. The systematic uncertainty of the flux scaled by E^3 due to the uncertainty of the energy scale of 22% is indicated by arrows. It has been used three power laws with free breaks between them. A continuation of the power law above the ankle to highest energies can be rejected with more than

Backup slide

- Photon energy threshold in the PRF:

$$E_{\gamma}^{th} = \frac{(m_{p,n,\Delta} + \Sigma m_{\pi})^2 - m_p^2}{2m_p} \quad (1)$$

- Making a lorentz transformation to the CRF where $E_{\gamma} = \epsilon = 2.5 \cdot 10^{-4} \text{meV}$

$$\epsilon = \gamma(E_{\gamma}^{th} - \beta p_{\gamma}^{th}) = \sqrt{\frac{1 - \beta}{1 + \beta}} E_{\gamma}^{th} \quad (2)$$

- Finding β , the relative velocity between PRF and CRF, the energy of the proton in the CRF can be calculated:

$$E_{CRF}^{th} = m_p \gamma = 1.068 \cdot 10^{20} \text{eV} \quad (3)$$

Backup slide

The Threshold energy for the other channels is of the same order:

Channel	$E_{\gamma}^{th}(PRF)$	$E_{th}(CRF)$
$p\gamma \rightarrow \pi^+\pi^-\pi^0p$	505.51 MeV	$3.73 \cdot 10^{20}$ eV
$p \rightarrow \Delta^{++}\pi^-$	533.35 MeV	$3.94 \cdot 10^{20}$ eV
$p\gamma \rightarrow \Delta^0\pi^+$	533.35 MeV	$3.94 \cdot 10^{20}$ eV
$p\gamma \rightarrow \pi^+\pi^-p$	320.63 MeV	$2.37 \cdot 10^{20}$ eV
$p\gamma \rightarrow \pi^0\pi^0p$	308.80 MeV	$2.28 \cdot 10^{20}$ eV
$p\gamma \rightarrow \pi^+\pi^-n$	321.35 MeV	$2.37 \cdot 10^{20}$ eV
$p\gamma \rightarrow \pi^0\pi^0\pi^0p$	492.32 MeV	$3.64 \cdot 10^{20}$ eV
$p\gamma \rightarrow \pi^+\pi^+\pi^-n$	513.02 MeV	$3.79 \cdot 10^{20}$ eV
$p\gamma \rightarrow \pi^+\pi^0\pi^0n$	507.38 MeV	$3.75 \cdot 10^{20}$ eV

Backup slide

- Pair production is responsible for the ankle:

$$p\gamma \rightarrow e^+e^-p \quad (4)$$

- Photon threshold energy in the PRF:

$$E_\gamma^{th}(PRF) = \frac{(m_p + 2m_e)^2 - m_p^2}{2m_p} \quad (5)$$

- Energy of the proton on the CRF:

$$E_\gamma^{th}(PRF) = 1.022MeV \longrightarrow E_p(CRF) = 7.54 \cdot 10^{17}eV \quad (6)$$

Backup slide

Absolute Calibration

- Drum-shaped light source mounted on the FD apertures.
- Provides a pulsed photon flux of known intensity
- All pixels are triggered.
- After calibration some pixels are checked with laser calibration.

Backup slide

- A laser pulse is shot vertically into the air with known intensity from the Central Laser Facility (CLF).
- Nitrogen laser is used (337 nm).
- The response of each pixel to the known (calculated) number of photons performs a calibration for those pixels.
- Overall calibration uncertainty $\approx 12\%$, dominated by atmospheric effects and probe calibration.

Backup slide

- Total background signal is sum of electronics (PMT and electronics noise) and sky brightness (airglow, moonlight, stars and planet light, twilight, artificial light).
- 3-5 ADC counts for electronics
- 20 ADC counts for cloudy nights
- 25-60 ADC counts for clear moonless nights.
- Several hundred ADC counts when moon is present.
- Optimal background: 25-60 ADC counts. Photon background flux of $100\text{-}250 \text{ photons } m^{-2} \text{ deg}^{-2} \mu s^{-1}$. These events are used for analysis.